# THREE-DIMENSIONAL SEEPAGE THROUGH SPATIALLY RANDOM SOIL

By D. V. Griffiths,[1] Member, ASCE, and Gordon A. Fenton,[2] Member, ASCE

**ABSTRACT:** This paper brings together random field generation and finite-element techniques to model steady seepage through a three-dimensional (3D) soil domain in which the permeability is randomly distributed in space. The analyses focus on the classical problem of steady seepage beneath a single sheet pile wall embedded in a finite layer of soil. The analyses treat the soil permeability as a spatially random property with specified mean, variance, and spatial correlation length. The influence of the spatial correlation or "scale of fluctuation" is given special consideration, since this aspect is not always included in probabilistic geotechnical analysis. The value of permeability assigned to each element comes from a lognormally distributed random field derived from local averages of a normally distributed random field. The local averaging allows the element dimensions to be rationally accounted for on a statistical basis. The influence of three-dimensionality is given particular emphasis and contrasted with results that are obtained using an idealized two-dimensional model. For the computationally intensive 3D finite-element analyses, strategies are described for optimizing the efficiency of the code in relation to memory and central processing unit requirements. Monte Carlo simulations are performed to establish statistics relating to quantities of interest to designers such as the flow rate. The potential value of this approach is emphasized by presenting the results in the context of reliability-based design.

## INTRODUCTION

The work presented in this paper brings together finite-element analysis and random field theory in the study of a three-dimensional (3D) boundary-value problem of steady seepage. The aim of the investigation is to observe the influence of soil variability on the expected value of 'output' quantities such as the flow rate. Smith and Freeze (1979a,b) were among the first to study the problem of confined flow through a stochastic medium using finite differences, in which two-dimensional (2D) examples of flow between parallel plates and beneath a single sheet-pile were presented. Recent developments in random field and finite-element methodology have led to further studies by the writers and others of steady seepage problems for a range of other 2D boundary-value problems (see, e.g., Fenton and Griffiths 1993; Griffiths and Fenton 1993; Benson 1993). See also Dagan (1989), Freeze et al. (1990), and Gelhar (1993) for a thorough review of related work in the area of flow through heterogeneous materials.

A conference on probabilistic methods in geotechnical engineering (Li and Lo 1993) highlighted some of the recent advances in this field. For example Mostyn and Li (1993) emphasized the importance of taking account of the spatial correlation of soil properties in probabilistic analyses. It was pointed out that the "vast majority of existing models do not do this," and although their particular application was the analysis of slope stability in which the random soil properties in question were the shear strength parameters, the same arguments could be applied to soil permeability in a seepage problem. White (1993) also described how early probabilistic analyses typically represented soil property uncertainty by the use of a single random variable that was varied from one calculation to the next.

The use of random fields (see, e.g., Vanmarcke 1984; Fenton and Vanmarcke 1990) was considered to be an important refinement, in that the soil property at each location within the soil mass was itself considered to be a random variable. A feature of the random field approach is that it appropriately takes into account the positive correlation that is observed between soil properties measured at locations that are "close" together.

The work presented herein extends the previous work of the writers to encompass 3D analysis. The earlier 2D model rested on the assumption of perfect correlation in the out-of-plane direction, an assumption no longer necessary with a 3D model.

## BRIEF DESCRIPTION OF FINITE-ELEMENT MODEL

In this paper a random field generator known as the Local Average Subdivision Method (LAS) devised by Fenton (1990) is combined with the power of the finite-element method for modeling spatially varying soil properties. The problem chosen for study is a simple boundary-value problem of steady seepage beneath a single sheet-pile wall penetrating a layer of soil. The variable soil property in this case is the soil perme-

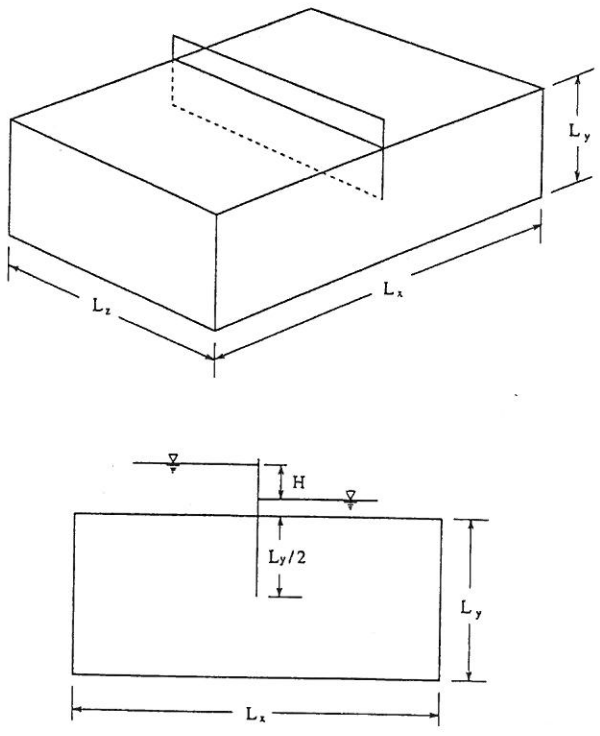


**FIG. 1. Isometric View of: (a) 3D Seepage Problem; (b) Elevation**

[1]Prof., Geomech. Res. Ctr., Colorado School of Mines, Golden, CO 80401-1887.

[2]Assoc. Prof., Dept. of Appl. Math., Tech. Univ. of Nova Scotia, Halifax, Nova Scotia, Canada B3J 2X4.

Note. Discussion open until July 1, 1997. To extend the closing date one month, a written request must be filed with the ASCE Manager of Journals. The manuscript for this paper was submitted for review and possible publication on March 22, 1995. This paper is part of the *Journal of Geotechnical and Geoenvironmental Engineering*, Vol. 123, No. 2, February, 1997. ©ASCE, ISSN 1090-0241/97/0002-0153–0160/$4.00 + $.50 per page. Paper No. 10365.

ability $K$ that is defined in the classical geotechnical sense as having units of $(L/T)$.

The overall dimensions of the problem to be solved are shown in Fig. 1(a,b). Fig. 1(a) shows an isometric view of the 3D flow regime, and Fig. 1(b) shows an elevation that corresponds to the 2D domain analyzed for comparison. In all results presented in this paper, the dimensions $L_x$ and $L_y$ and the depth of wall embedment $(L_y/2)$ were held constant while the third dimension $L_z$ was gradually increased to monitor the effects of three-dimensionality.

The finite-element program used for the solutions of Laplace's equation presented in this paper was obtained by combining Programs 5.9 and 7.0 from the modular code published in the text by Smith and Griffiths (1988). In all analyses presented here, a uniform mesh of cubic eight-node brick elements with a side length of 0.2 was used with 32 elements in the $x$-direction ($L_x = 6.4$), 16 elements in the $y$-direction ($L_y = 3.2$), and up to 16 elements in the $z$-direction ($L_z = 0.8$, 1.6, and 3.2). A time-saving feature of "brick" elements (i.e., all sides meet at 90° to each other) such as those used in the present study, is that their conductivity matrices are easily computed explicitly without the need for numerical integration. It should be noted that a general eight-node hexahedral element requires evaluation of the function being integrated at eight internal Gauss points. The brick element, on the other hand, allows the variables to be separated and an analytical integration to be performed.

Using the local freedom numbering indicated in Fig. 2, the symmetric conductivity matrix $\mathbf{k}_i$ of the $i$th element of side length $a$ and isotropic permeability $K_i$ is given by (upper triangle only shown for clarity)

$$\mathbf{k}_i = \frac{K_i a}{12}\begin{bmatrix} 4 & 0 & -1 & 0 & 0 & -1 & -1 & -1 \\ & 4 & 0 & -1 & -1 & 0 & -1 & -1 \\ & & 4 & 0 & -1 & -1 & 0 & -1 \\ & & & 4 & -1 & -1 & -1 & 0 \\ & & & & 4 & 0 & -1 & 0 \\ & & & & & 4 & 0 & -1 \\ & & & & & & 4 & 0 \\ & & & & & & & 4 \end{bmatrix} \quad (1)$$

Within each mesh, the freedoms were numbered to minimize bandwidths of the global conductivity matrix together with a "skyline" storage strategy and Cholesky factorization to solve the simultaneous equations (see, e.g., page 78 of Smith and Griffiths 1988). The skyline approach was found to run faster than conventional (constant band-width) methods as well as giving substantial savings on memory requirement; a particularly important consideration in 3D analysis.

The code now has the additional option of using an iterative Algebraic Multigrid Method (see, e.g., Vaněk et al. 1994) for solving simultaneous equations. This method shows considerable promise for speeding up the solution process, and the time saving over direct solution strategies improves further still as the number of equations increases. It is anticipated that iterative approaches of this type will become the standard solution method for large 3D flow systems in future studies.

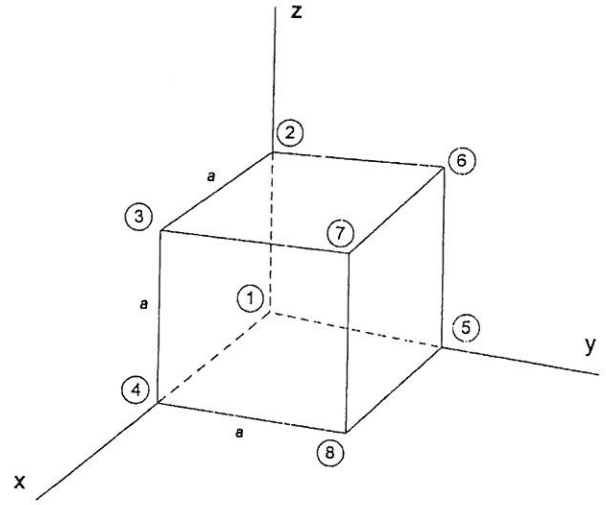


**FIG. 2. Local Node Numbering for Eight-Node "Brick" Laplacian Element**

## BRIEF DESCRIPTION OF RANDOM FIELD MODEL

Field measurements of permeability have indicated an approximately lognormal distribution (see, e.g., Hoeksema and Kitanidis 1985; Sudicky 1986). The same distribution has therefore been adopted for the simulations generated in this paper.

Essentially, the permeability field is obtained through the transformation

$$K_i = \exp\{\mu_{\ln k} + \sigma_{\ln k} G_i\} \quad (2)$$

in which $K_i$ = permeability assigned to the $i$th element; $G_i$ = local average of a standard Gaussian random field, $G$, over the domain of the $i$th element; and $\mu_{\ln k}$ and $\sigma_{\ln k}$ = mean and standard deviation of the logarithm of $K$, obtained from the prescribed mean and standard deviation $\mu_k$ and $\sigma_k$ via the transformations

$$\mu_k = \exp\left\{\mu_{\ln k} + \frac{1}{2}\sigma^2_{\ln k}\right\}; \quad \sigma^2_k = (\mu_k)^2(\exp\{\sigma^2_{\ln k}\} - 1) \quad (3, 4)$$

The LAS technique (Fenton 1990; Fenton and Vanmarcke 1990) generates realizations of the local averages $G_i$ that are derived from the isotropic random field $G$ having zero mean, unit variance, and a Gauss-Markov spatial correlation function

$$\rho(\tau) = \exp\left\{-\frac{2}{\theta_k}|\tau|\right\} \quad (5)$$

where $|\tau|$ = distance between points in the field; and $\theta_k$ = scale of fluctuation. The term "realization" in this context refers to a single generation of the random field and the subsequent finite-element analysis of that field. A Monte Carlo process involves a large number of realizations that eventually enable statistical statements to be made about the output quantities of interest.

Loosely speaking, the scale of fluctuation is the distance over which points in the field are significantly correlated. For example, from (5), for $\tau < \theta$, the correlation coefficient $\rho > 0.13$. As the scale of fluctuation goes to infinity, $G_i$ becomes equal to $G_j$ for all elements $i$ and $j$—that is, the field of permeabilities tends to become uniform on each realization (but each realization can still be quite different). At the other extreme, as the scale of fluctuation goes to zero, $G_i$ and $G_j$ become independent for all $i \neq j$—the soil permeability changes rapidly from point to point.

In the 3D analyses presented in this paper, the scales of fluctuation in all directions are taken to be equal (isotropic) for simplicity. Although beyond the scope of this paper, it should be noted that for a layered soil mass the horizontal scales of fluctuation are generally larger than the vertical scale due to the natural stratification of many soil deposits. A limitation of the 2D models considered previously was that the out-of-plane scale of fluctuation was assumed infinite—soil properties constant in this direction—which is equivalent to specifying that the streamlines must remain in the plane of the analysis. This was clearly a deficiency and motivated the present work, in which no such assumptions are made.

A comparison between different methods of random field

generation, including the LAS method, has been presented by Fenton (1994).

## SUMMARY OF RESULTS FROM SEEPAGE ANALYSES

A Monte Carlo approach to the seepage problem was adopted in which, for each set of input statistics ($\mu_k$, $\sigma_k$, $\theta_k$) (or equivalently, $\mu_{\ln k}$, $\sigma_{\ln k}$, $\theta_{\ln k}$) and mesh geometry ($L_z$), 1,000 realizations were performed.

The main output quantities of interest from each realization in this problem are the total flow rate through the system $Q$ and the exit gradient $i_e$. The rather more complicated issues relating to analysis of the exit gradient are beyond the scope of the present work and will be analyzed in a future publication.

In this paper, therefore, the writers focus on the flow rate. Following Monte Carlo simulations, the mean and standard deviation of $Q$ were computed and presented in nondimensional form by representing $Q$ in terms of a normalized flow rate $\bar{Q}$ thus

$$\bar{Q} = Q/(H\mu_k L_z) \tag{6}$$

where $H$ = total head loss across the wall. In all the calculations performed in this study, $H$ was set to unity since it has simple linear influence on the flow rate $Q$. Division by $L_z$ has the effect of expressing the average flow rate over one unit of thickness in the $z$-direction enabling a direct comparison to be made with the 2D results.

The following parametric variations were implemented for fixed $\mu_k = 1 \times 10^{-5}$, $L_x = 6.4$, and $L_y = 3.2$:

$$\sigma_k/\mu_k = 0.125, 0.25, 0.5, 1, 2, 4 \text{ and } 8 \tag{7a}$$

$$\theta_k = 1, 2, 4, 8 \text{ and } \infty \text{ (analytical)} \tag{7b}$$

$$L_z = 0.8, 1.6 \text{ and } 3.2 \tag{7c}$$

As the coefficient of variation of the input permeability ($COV_k = \sigma_k/\mu_k$) was increased, the mean estimated normalized flow rate, $m_Q$, was observed to fall consistently from its deterministic value (assuming constant permeability = $\mu_k$ throughout) of $\bar{Q}_{det} \approx 0.47$ as shown in Fig. 3(a) for the case where $L_z/L_y = 1$. The fall in $m_{\bar{Q}}$ was steepest for small values of the scale of fluctuation $\theta_k$; however, as $\theta_k$ was increased, $m_{\bar{Q}}$ tended toward the deterministic result that would be expected for a strongly correlated permeability field ($\theta_k \to \infty$).

The reduction in the expected flow rate with increased permeability variance but fixed mean has been described as "counter-intuitive" by some observers. The explanation lies in the fact that in a continuous flow regime such as the one modeled here, flow must be occurring in every region of the domain, so the greater the permeability variance, the greater the volume of low permeability material that must be negotiated along any flow path. In an extreme case of "series" flow down a 1D pipe of varying permeability cells, the effective permeability is given by the harmonic mean of the permeability values, which is heavily dependent on the lowest permeability encountered. The other extreme of "parallel" flow leads to the arithmetic mean. The 3D example considered here is a complex combination of parallel and series flow that leads to an effective permeability more closely approximated by the geometric mean (see, e.g., Griffiths et al. 1994) that is always smaller than the arithmetic mean (but not as small as the harmonic mean).

Fig. 3(b) shows the estimated standard deviation of the normalized flow rate, $s_{\bar{Q}}$, for the same geometry. For small $\theta_k$ very little variation in $\bar{Q}$ was observed, even for high coefficients of variation. This is understandable if one thinks of the total flow through the domain as effectively an averaging process —high flow rates in some regions are offset by lower flow rates in other regions. It is well known in statistics that the variance of an average decreases linearly with the number of independent samples used in the average. In the random field context, the "effective" number of independent samples increases as the scale of fluctuation decreases, thus the decrease in variance in flow rate is to be expected. Conversely, when the scale of fluctuation is large, the variance in the flow rate

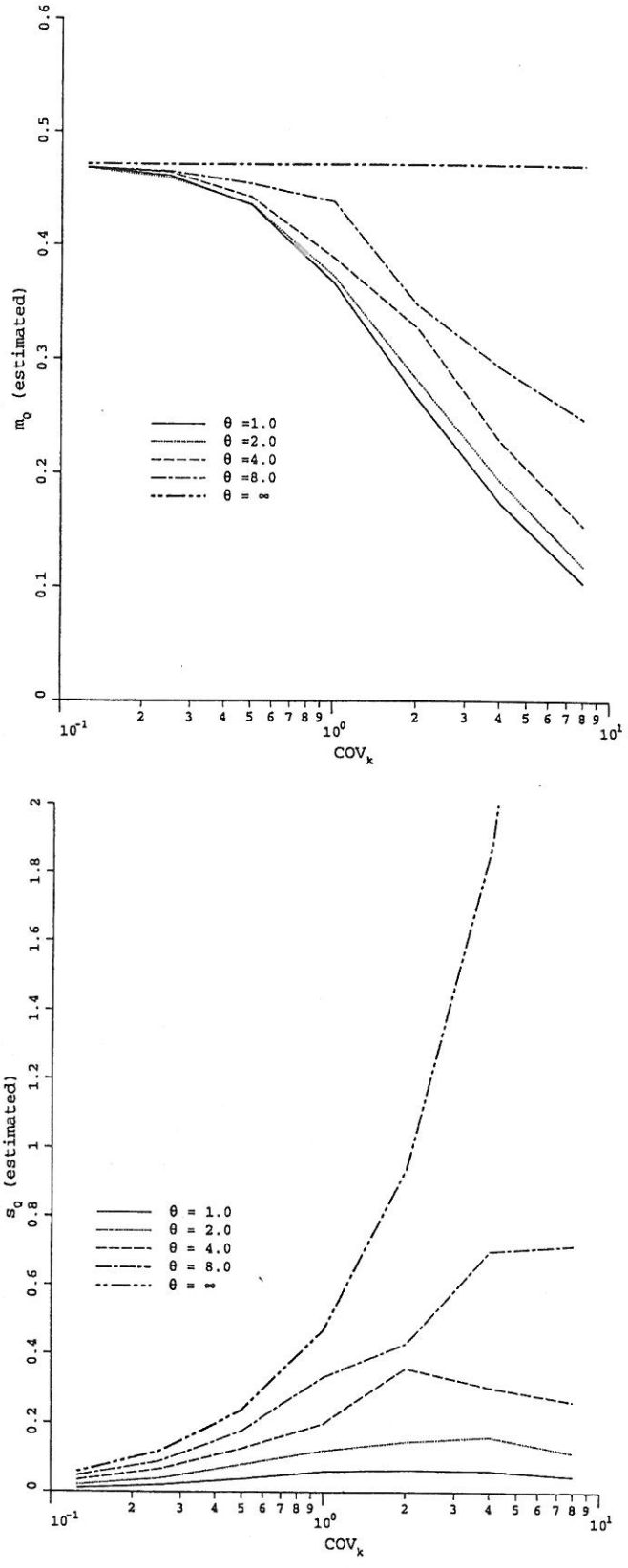


**FIG. 3. Influence of $\theta_k$ on Statistics of Normalized Flow Rate ($L_z/L_y = 1$): (a) Mean; (b) Standard Deviation**

is also expected to be larger—there is less "averaging" variance reduction within each realization. The maximum flow rate variance is obtained when the field becomes completely correlated ($\theta_k = \infty$), in which case the permeability is uniform at each realization. Since the flow rate is proportional to the (uniform) permeability in this case, the flow rate variance exactly follows that of the permeability, thus

$$\sigma_Q = \frac{\sigma_k}{\mu_k} \bar{Q}_{det} \tag{8}$$

It is instructive at this stage to give further consideration to the estimated statistics of flow rate. $\mu_{\ln \bar{Q}}$ is estimated by $m_{\ln \bar{Q}}$ and $\sigma_{\ln \bar{Q}}$ by $s_{\ln \bar{Q}}$, where $m_{\ln \bar{Q}}$ and $s_{\ln \bar{Q}}$ are obtained from the log-flow rates following $n$ realizations of the Monte Carlo process. Assuming that the flow rates are lognormally distributed, the log estimators can then be transformed into direct estimates using the equations

$$m_{\bar{Q}} = \exp\left\{m_{\ln \bar{Q}} + \frac{1}{2} s^2_{\ln \bar{Q}}\right\}; \quad s^2_{\bar{Q}} = (m_{\bar{Q}})^2(\exp\{s^2_{\ln \bar{Q}}\} - 1) \tag{9, 10}$$

In general, estimates based on log data and then transformed will be different from estimates based on the raw data unless the data exactly fit the lognormal distribution. As will be seen, however, the computed flow rates in this study appear to closely follow the lognormal distribution.

To assess the accuracy of these estimators in terms of their reproducibility, the standard deviation of the estimators can be related to the number of simulations of the Monte Carlo process, assuming ln $\bar{Q}$ is normally distributed, as follows (in this study $n$ = 1,000):

$$\sigma_{m_{\ln \bar{Q}}} = \sqrt{\frac{1}{n}}\, s_{\ln \bar{Q}} \approx 0.032 s_{\ln \bar{Q}} \tag{11}$$

$$\sigma_{s^2_{\ln \bar{Q}}} = \sqrt{\frac{2}{n-1}}\, s^2_{\ln \bar{Q}} \approx 0.045 s^2_{\ln \bar{Q}} \tag{12}$$

Due to the variance reduction arising from averaging, the variance of the estimator, $s_{\bar{Q}}$, will increase towards the result given by (12) as the scale of fluctuation increases, that is, (12) is an upper bound on the estimator variance. This can be seen in both Fig. 3(a,b) where the curves for larger $COV_k$ and $\theta_k$ show increasingly erratic behavior. In these cases, more than 1,000 realizations may be required to obtain accuracy similar to that obtained for smaller $\theta_k$.

Fig. 4(a,b) shows the influence of three-dimensionality on the estimated mean and standard deviation of $\bar{Q}$ by comparing results with gradually increasing numbers of elements in the $z$-direction. Also included in Fig. 4(a,b) is the 2D result that implies an infinite scale of fluctuation in the $z$-direction and allows no flow out of the plane of the analysis. The particular cases shown correspond to a fixed scale of fluctuation $\theta_k = 1$.

Compared with 2D analysis, three dimensions allows the flow greater freedom to "avoid" the low permeability zones. This results in a less steep reduction in the expected flow rate with increasing $COV_k$ as shown in Fig. 4(a). There is also a corresponding reduction in the variance of the expected flow rate as the third dimension is elongated as shown in Fig. 4(b). In summary, the effect of allowing flow in three dimensions is to increase the averaging effect analyzed previously within each realization. The difference between the 2D and 3D results is not that great, however, and it could be argued that a 2D analysis is a reasonable first approximation to the "true" behavior in this case. It should be noted however, that the 2D approximation will tend to underestimate the expected flow through the system that is an unconservative result from the point of view of engineering design.

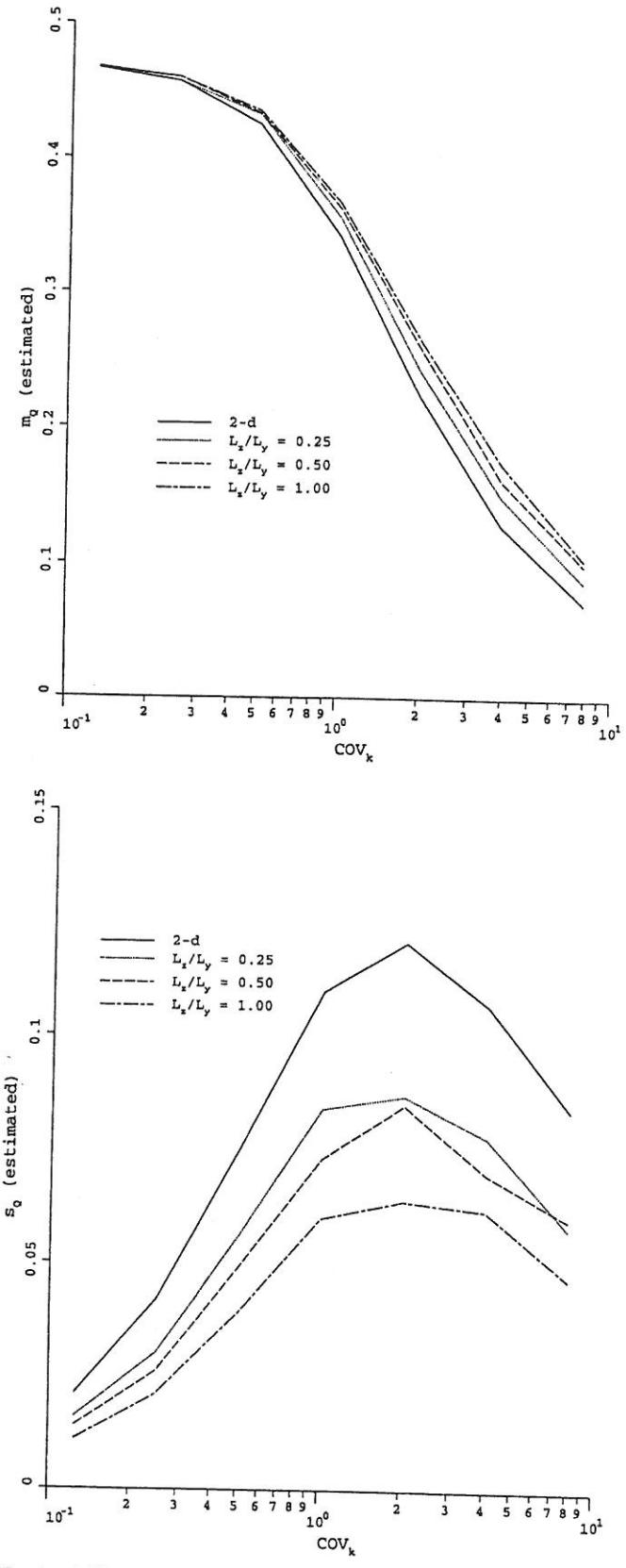


**FIG. 4. Influence of $L_z/L_y$ on Statistics of Normalized Flow Rate ($\theta_k$ = 1): (a) Mean; (b) Standard Deviation**

## Interpretation of Results for Reliability-Based Design

One of the main objectives of stochastic analyses such as those described in this paper is to enable statements to be made relating to the probability of certain events occurring. Reliability-based design depends on this approach, so consider again the case of flow rate prediction beneath a water retaining

structure. Deterministic approaches using fixed values of permeability throughout the finite element mesh will lead to a particular value of the flow rate that can then be factored (i.e., scaled up) as deemed appropriate by the designers. Provided this factored value is less than the maximum acceptable flow rate, the design is considered to be acceptable and in some sense "safe." Although the designer would accept that there is still a small possibility of failure, this is subjective and no attempt is made to quantify the risk.

The stochastic approach, on the other hand, is more realistic in recognizing that even in a "well-designed" system, there will always be a possibility that the maximum acceptable flow rate could be exceeded if an unfortunate combination of soil properties should occur. The designers then have to make a quite different decision relating to how high a "probability of failure" would be acceptable.

Figs. 5 and 6 show typical histograms of the flow rate following 1,000 realizations for the cases where $L_z/L_y = 1.00$,

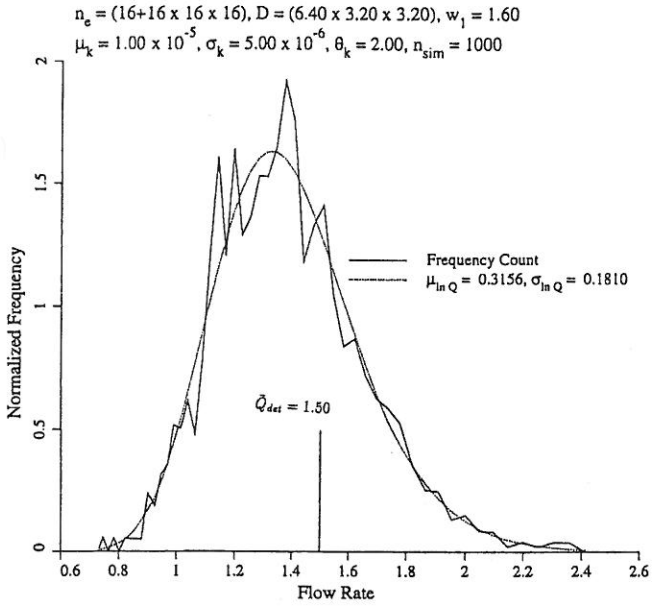


**FIG. 5. Histogram of Computed Flow Rates Following 1,000 Realizations ($COV_k = 0.5$, $\theta_k = 2.00$); 3D Stochastic Analysis of Ground-Water Flow—One Wall Case**

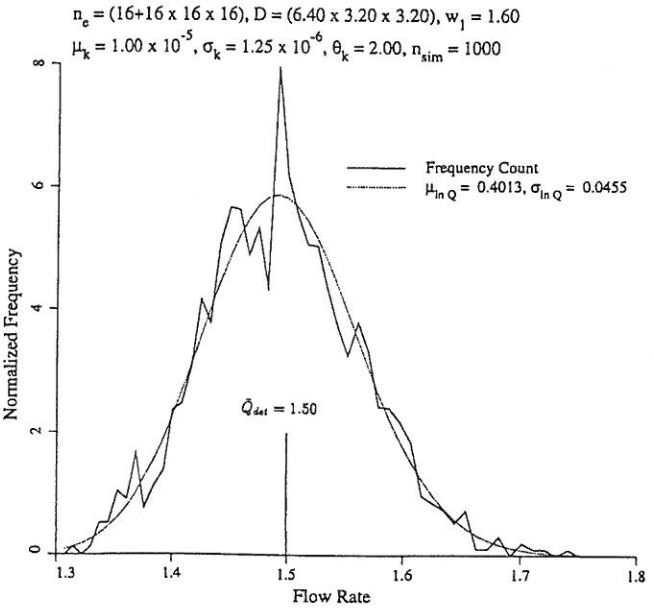


**FIG. 6. Histogram of Computed Flow Rates Following 1,000 Realizations ($COV_k = 0.125$, $\theta_k = 2.00$); 3D Stochastic Analysis of Ground-Water Flow—One Wall Case**

$\theta_k = 2.00$, and $COV_k = 0.50$ and $COV_k = 0.125$, respectively. They are both seen to match well with the hatched lines representing the fitted lognormal distribution using the estimated mean and standard deviation values computed from the simulations. The mean and standard deviation of the underlying normal distribution of ln $\bar{Q}$ is given in each figure. The histograms have been normalized such that the area beneath the curves equals unity. This type of normalization enables probabilities to be easily computed.

The total deterministic flow rate through the 3D geometry that would have occurred if the permeability was constant and equal to unity is given by

$$\bar{Q}_{det} = 0.47 \times 3.2 = 1.50 \tag{13}$$

where $L_z = 3.2$ is the width of the flow problem in the $z$-direction and 0.47 represents the deterministic flow per unit width based on a 2D analysis in the $x$-$y$ plane [see Fig. 1(b)]. This value can be compared directly with the histograms in Figs. 5 and 6 and it can be seen that the deterministic mean flow rate is shifted to the right of the distribution mean when $COV_k = 0.50$ (Fig. 5) but is quite close to the distribution mean when $COV_k = 0.125$ (Fig. 6).

For reliability-based design, a major objective of this type of analysis would be to estimate the probability that the deterministic flow rate underestimates the "true" flow rate. Such an underestimation would imply an "unsafe" design and should have an appropriately "low" probability. The actual value of an acceptable design "probability of failure" is beyond the scope of this paper, however, since this depends on a number of factors, not least the importance of the water retaining structure in relation to safety and infrastructure downstream.

Referring to the particular case shown in Fig. 5, the estimated probability that the deterministic flow rate underestimates the "true" flow rate is given by the following calculations, which assume a normal distribution of ln $\bar{Q}$:

$$P(\bar{Q} > \bar{Q}_{det}) = 1 - \Phi\left(\frac{\ln 1.50 - 0.3156}{0.1810}\right) = 0.298 \tag{14}$$

where $\mu_{\ln \bar{Q}} = 0.3156$ and $\sigma_{\ln \bar{Q}} = 0.1810$ are the parameters of the fitted distribution shown in Fig. 5 and $\Phi(\cdot)$ is the standard normal cumulative distribution function. A similar calculation applied to the data in Fig. 6 leads to

$$P(\bar{Q} > \bar{Q}_{det}) = 0.405 \tag{15}$$

and for a range of different $COV_k$ values with a constant scale of fluctuation given by $\theta_k = 2.00$, the probability of an "unsafe" design has been plotted as a function of $\log_{10} COV_k$ in Fig. 7.

Fig. 7 shows that a deterministic calculation based on the mean permeability will always lead to a conservative estimate of the flow rate [i.e., $P(\bar{Q} > \bar{Q}_{det}) < 50\%$]. As the coefficient of variation of the permeability increases, however, the probability that the true flow rate will exceed the deterministic value decreases. For the range of $COV_k$ values considered, the probability varied from less than 2% for $COV_k = 8$ to a probability of 40% for $COV_k = 0.125$. In the latter case, however, the standard deviation of the computed flow also becomes small, so the range of flow-values more resembles a normal distribution than lognormal. In the limit as $COV_k \to 0$, the solution tends to the deterministic value, but in probabilistic terms this implies an equal likelihood of the true flow rate falling on either side of the predicted value. Hence the curve in Fig. 7 tends to a probability of 50% for small values of $COV_k$.

These results are reassuring from a design viewpoint, because they indicate that the traditional approach leads to a

conservative estimate of the flow rate—the more variable the soil, the more conservative the prediction. This observation is made with the knowledge that permeability is considered one of the most variable of soil properties with coefficient of variation values ranging as high as three (see, e.g., Lee et al. 1983, Kulhawy et al. 1991).

The sensitivity of the probability $P(\bar{Q} > \bar{Q}_{det})$ to variations in the scale of fluctuation $\theta_k$ is shown in Fig. 8. The coefficient of variation of the soil permeability is maintained at a constant value given by $COV_k = 0.50$ and the scale of fluctuation is varied in the range $0.5 < \theta_k < 8$. This result shows that as the scale of fluctuation increases the probability of the true flow rate being greater than the deterministic value also increases, although its value is always less than 50%. In the limit, as $\theta_k \rightarrow \infty$, each realization of the Monte Carlo process assumes a perfectly correlated field of permeability values. In this case, the flow rate distribution is identical to the permeability distribution with a mean equal to the flow rate that would have been computed using the mean permeability. The probability

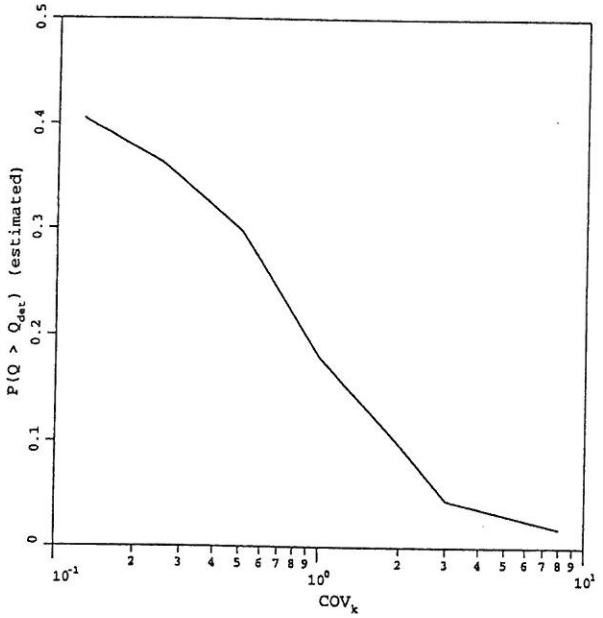


**FIG. 7. Probability of "Unsafe" Design Plotted Against $COV_k$ ($\theta_k = 2.00$, $L_z/L_y = 1.00$)**

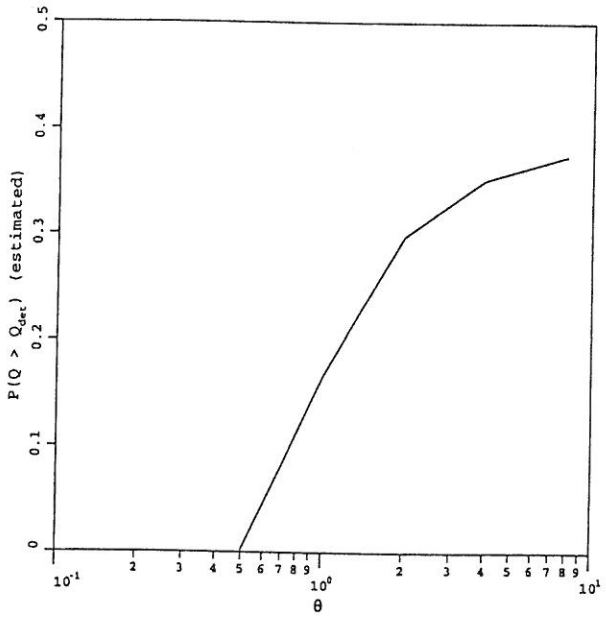


**FIG. 8. Probability of "Unsafe" Design Plotted Against $\theta_k$ ($COV_k = 0.50$, $L_z/L_y = 1.00$)**

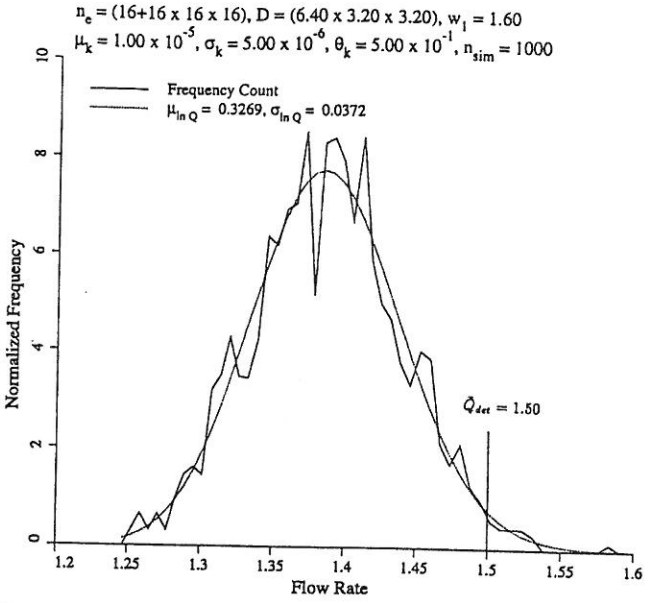


**FIG. 9. Histogram of Computed Flow Rates Following 1,000 Realizations ($COV_k = 0.50$, $\theta_k = 0.50$); 3D Stochastic Analysis of Ground-Water Flow—One Wall Case**

in this case therefore tends to be 50%. As $\theta_k$ is reduced however, the probability of the true flow rate being greater than the deterministic value reduces quite steeply and approaches zero for $\theta = 0.5$. The actual value of $\theta$ in the field will not usually be well established (except perhaps in the vertical direction where sampling is continuous), so sensitivity studies help to give a feel for the importance of this parameter. For further information on soil property correlation, the interested reader is referred to Lumb (1966), Asaoka and Grivas (1982), DeGroot and Baecher (1993), and de Marsily (1985).

The results in Fig. 8 corresponding to very low probabilities [e.g., $P(\bar{Q} > \bar{Q}_{det} < 0.01)$] must be interpreted cautiously however, as more than the 1,000 realizations of the Monte Carlo process used in this paper would be needed for accuracy in this range. In addition, low probabilities can be significantly in error when estimated parameters are used to describe the distribution. Qualitatively, the fall in probability with decreasing $\theta_k$ is shown well in the histogram of Fig. 9, where for the case of $\theta_k = 0.5$, the deterministic flow rate lies well within the right hand tail of the distribution leading to $P(\bar{Q} > \bar{Q}_{det}) \approx 0.002$.

## Comment on Computer Timings

The results presented in this paper were run on a DEC 3000 Model 400 workstation. A summary of the total CPU time consumed by the various analyses is presented in Table 1. The "Timing" column is expressed in nondimensional form with respect to an equivalent 2D analysis with the same mesh density in the $xy$-plane.

As mentioned previously, these timings were obtained using direct solution methods for the simultaneous equations that result from each realization. It is anticipated that the use of iterative solvers (e.g., Vaněk et al. 1994) will considerably

**TABLE 1. Comparison of Timings from 2D and 3D Analyses**

| Dimension (1) | Timing (2) |
|---|---|
| 2D | 1 |
| $L_z/L_y = 0.25$ | 49 |
| $L_z/L_y = 0.50$ | 239 |
| $L_z/L_y = 1.00$ (direct) | 1,463 |
| $L_z/L_y = 1.00$ (iterative) | 408 |

improve these timings, especially for large 3D modeling. Initial indications are that even without any code optimization, improvements of up to a factor of four can be achieved for the full 3D case ($L_z/L_y = 1$) with approximately 10,000 degrees of freedom. Greater improvements are anticipated in the future helping to bring serious 3D analyses of this type within the domain of a desktop workstation environment.

## CONCLUDING REMARKS

In this paper, 3D random field and finite-element methods have been combined in the study of steady seepage beneath a single sheet-pile wall embedded in a layer of random soil. An extensive parametric study has been performed in which the coefficient of variation and the spatial correlation of soil permeability have been systematically varied to observe their influence on the mean and standard deviation of the flow rate through the system. In addition, the influence of three-dimensionality has been investigated by gradually increasing the width of the model in the direction of the wall. In all cases, results were compared with those that would have been obtained using a 2D analysis.

For low to moderate values of the scale of fluctuation ($\theta <$ 8), the expected value of the flow rate was found to fall consistently as the coefficient of variation of the input permeability was increased. The explanation lies in the fact that in a continuous flow regime such as the one modeled here, the low permeability zones cannot be "avoided," so the greater the permeability variance, the greater the volume of low permeability material that must be negotiated and the lower the flow rate. For higher values of the scale of fluctuation ($\theta > 8$), the normalized flow rate mean tended to the deterministic value. The standard deviation of the flow rate was shown to consistently increase with the scale of fluctuation and the standard deviation of the input permeability, but within the bounds defined analytically for the limiting case of perfect correlation.

The influence of three-dimensionality was to reduce the overall "randomness" of the results observed from one realization to the next. This had the effect of increasing the expected flow rate and reducing the variance of the flow rate over those values observed from a 2D analysis with the same input statistics. Although unconservative in the estimation of flow rates, there was not a great difference between the 2D and 3D results, suggesting that the simpler and less expensive 2D approach may give acceptable accuracy for the cases considered.

Some of the results were reinterpreted from a reliability viewpoint and indicated that if the flow rate was computed deterministically using the mean permeability, the probability of the true flow being greater would always be less than 50%. This probability fell to even smaller values as the variance of the input permeability was increased or the scale of fluctuation was reduced, implying that a deterministic prediction of flow rate based on the mean permeability would always be conservative on average.

## ACKNOWLEDGMENTS

The writers acknowledge the partial support of NATO Collaborative Research Grant No. 911007, the SERC (UK) Research Grant No. GR/H44066, and the NSERC (Canada) Grant No. OPG0105445.

## APPENDIX I. REFERENCES

Asaoka, A., and Grivas, D. A. (1982). "Spatial variability of the undrained strength of clays." *J. Geotech. Engrg.*, ASCE, 108(5), 743–756.

Benson, C. H. (1993). "Probability distributions for hydraulic conductivity of compacted soil liners." *J. Geotech. Engrg.*, ASCE, 119(3), 471–486.

Dagan, G. (1989). "Flow and transport in porous formations." Springer-Verlag KG, Berlin, Germany.

DeGroot, D. J., and Baecher, G. B. (1993). "Estimating autocovariance of in-situ soil properties." *J. Geotech. Engrg.*, ASCE, 119(1), 147–166.

de Marsily, G. (1985). "Spatial variability of properties in porous media: A stochastic approach." *Advances in transport phenomena in porous media*, J. Bear and M. Y. Corapcioglu, eds., NATO Advanced Study Inst. on Fundamentals of Transport Phenomena in Porous Media, Boston, Mass., 719–769.

Fenton, G. A. (1990). "Simulation and analysis of random fields," PhD thesis, Princeton Univ., Princeton, N.J.

Fenton, G. A. (1994). "Error evaluation of three random-field generators." *J. Engrg. Mech.*, ASCE, 120(12), 2478–2496.

Fenton, G. A., and Griffiths, D. V. (1993). "Statistics of flow through a simple bounded stochastic medium." *Water Resour. Res.*, 29(6), 1825–1830.

Fenton, G. A., and Vanmarcke, E. H. (1990). "Simulation of random fields via local average subdivision." *J. Engrg. Mech.*, ASCE, 116(8), 1733–1749.

Freeze, R. A., Massman, J., and Smith, L. (1990). "Hydrogeological decision analysis: 1. a framework." *Ground Water*, 28(5), 738–766.

Gelhar, L. W. (1993). *Stochastic subsurface hydrology*. Prentice-Hall, Inc., Englewood Cliffs, N.J.

Griffiths, D. V., and Fenton, G. A. (1993). "Seepage beneath water retaining structures founded on spatially random soil." *Géotechnique*, London, England, 43(4), 577–587.

Griffiths, D. V., Paice, G. M., and Fenton, G. A. (1994). "Finite element modeling of seepage beneath a sheet pile wall in spatially random soil." *IACMAG 94*, H. J. Siriwardane and M. M. Zaman, eds., A. A. Balkema, Rotterdam, The Netherlands, 1205–1209.

Hoeksema, R. J., and Kitanidis, P. K. (1985). "Analysis of the spatial structure of properties of selected aquifers." *Water Resour. Res.*, 21(4), 563–572.

Kulhawy, F. H., Roth, M. J. S., and Grigoriu, M. D. (1991). "Some statistical evaluations of geotechnical properties." *Proc., ICASP6, 6th Int. Conf. Appl. Statistical Problems in Civ. Engrg.*

Lee, I. K., White, W., and Ingles, O. G. (1983). *Geotechnical engineering*. Pitman Publishing, Ltd., London, England.

Li, K. S., and Lo, S.-C. R., eds. (1993). *Probabilistic methods in geotechnical engineering*. A. A. Balkema, Rotterdam, The Netherlands.

Lumb, P. (1966). "The variability of natural soils." *Can. Geotech. J.*, 3(2), 74–97.

Mostyn, G. R., and Li, K. S. (1993). "Probabilistic slope stability—state of play." *Proc., Conf. Probabilistic Methods Geotech. Engrs.*, K. S. Li and S.-K. R. Lo, eds., A. A. Balkema, Rotterdam, The Netherlands, 89–110.

Smith, I. M., and Griffiths, D. V. (1988). *Programming the finite element method*, 2nd Ed., John Wiley & Sons, Inc., New York, N.Y.

Smith, L., and Freeze, R. A. (1979). "Stochastic analysis of steady state groundwater flow in a bounded domain. 1. one-dimensional simulations." *Water Resour. Res.*, 15(3), 521–528.

Smith, L., and Freeze, R. A. (1979b). "Stochastic analysis of steady state groundwater flow in a bounded domain. 2. Two-dimensional simulations." *Water Resour. Res.*, 15(6), 1543–1559.

Sudicky, E. A. (1986). "A natural gradient experiment on solute transport in a sand aquifer: spatial variability of hydraulic conductivity and its role in the dispersion process." *Water Resour. Res.*, 22(13), 2069–2083.

Vaněk, P., Mandel, J., and Brezina, M. (1994). "Algebraic multi grid by smoothed aggregation for second and fourth order elliptic problems." *Proc., GANM Workshop on Multilevel Techniques*, Meissdorf.

Vanmarcke, E. H. (1984). *Random fields: analysis and synthesis*. MIT Press, Cambridge, Mass.

White, W. (1993). "Soil variability: characterisation and modelling." *Proc., Conf. Probabilistic Methods in Geotech. Engrg.*, K. S. Li and S.-C. R. Lo, eds., A. A. Balkema, Rotterdam, The Netherlands, 111–120.

## APPENDIX II. NOTATION

*The following symbols are used in this paper:*

$a$ = finite-element side length;
$COV_k$ = coefficient of variation ($\sigma_k/\mu_k$);
$G$, $G_i$ = local average over $i$th element of standard Gaussian field;
$H$ = head difference;
$i_e$ = exit gradient;
$\mathbf{k}_i$ = conductivity matrix of the $i$th element;

$K$, $K_i$ = soil permeability of the $i$th element;
$L_x$, $L_y$, $L_z$ = mesh dimensions;
$m_{\tilde{Q}}$ = estimated mean of normalized flow rate;
$P(\tilde{Q} < \tilde{Q}_{det})$ = probability that "true" flow rate exceeds deterministic value;
$Q$ = flow rate;
$\tilde{Q}$ = normalized flow rate;
$\tilde{Q}_{det}$ = normalized deterministic flow rate;
$s_{\tilde{Q}}$ = estimated standard deviation of normalized flow rate;
$\theta$ = scale of fluctuation of permeability;
$\mu_k$ = target mean of permeability;
$\mu_{\ln k}$ = mean of logarithm of permeability;
$\mu_{\tilde{Q}}$ = mean of normalized flow rate;
$\mu_{\ln \tilde{Q}}$ = mean of logarithm of normalized flow rate;
$\sigma_k$ = standard deviation of permeability;
$\sigma_{\ln k}$ = standard deviation of logarithm of permeability;
$\sigma_{\tilde{Q}}$ = standard deviation of normalized flow rate;
$\sigma_{\ln \tilde{Q}}$ = standard deviation of logarithm of normalized flow rate;
$\rho$ = correlation function; and
$\tau$ = distance between two points in field.